physica **pss** status solidi **a**

www.pss-a.com

applications and materials science

Metal-face InAlN/AlN/GaN high electron mobility transistors with regrown ohmic contacts by molecular beam epitaxy

Jia Guo[1], Yu Cao[1], Chuanxin Lian[1], Tom Zimmermann[1], Guowang Li[1], Jai Verma[1], Xiang Gao[2], Shiping Guo[2], Paul Saunier[3], Mark Wistey[1], Debdeep Jena[1], and Huili (Grace) Xing*,[1]

[1] Department of Electrical Engineering, University of Notre Dame, Notre Dame, IN 46556, USA
[2] IQE RF LLC, Somerset, NJ 08873, USA
[3] Triquint Semiconductor Inc., Richardson, TX 75080, USA

* Corresponding author: e-mail hxing@nd.edu, Phone: +1 574 631 9108, Fax: +1 574 631 4393

Ohmic regrowth by molecular beam epitaxy (MBE) has been investigated for metal-face InAlN/AlN/GaN high electron mobility transistors (HEMTs) for the first time. Using SiO_2 mask n^+-GaN was regrown in the source/drain region while deposition on the mask was lifted off in buffered HF after regrowth. The lowest contact resistance measured was $0.40 \pm 0.23\ \Omega$ mm by the transmission line method (TLM) in this initial study. The peak output current density of 1.25 A/mm at $V_{gs} = 3$ V and extrinsic transconductance of 264 mS/mm at $V_{ds} = 5$ V were observed in 500-nm gate length InAlN/Al/GaN HEMTs passivated by SiN with regrowth contacts.

1 Introduction High-power high-frequency performance has been demonstrated for strained (Al, Ga)N/GaN as well as lattice matched InAlN/GaN based high electron mobility transistors (HEMTs) due to its wide bandgap, high electron velocity and large 2-dimensional electron gas (2DEGs) induced by polarization effects at the hetero-interface [1–4]. For all applications, it is highly desirable to keep the ohmic contact resistance as low as possible to minimize parasitic losses and improve device reliability. However, due to its wide bandgap, low contact resistances are difficult to achieve on (Al, Ga, In)N/GaN HEMTs. Conventionally, ohmic contacts for (Al, GaN, In)N/GaN HEMTs have been made by alloying Ti/Al/Ni/Au stacks at high temperatures. During annealing, severe lateral diffusion of ohmic metals and its rough surface makes it difficult to accurately place the gate relative to the source to drain. Non-alloyed or low-temperature-alloyed ohmic contact schemes have been also studied, including ohmic regrowth [5, 6], ion implantation [7], recessed ohmics [8], plasma pre-treatment [9], etc. Among all the reported methods, lowest contact resistances were obtained using regrowth: $R_c = 0.027\ \Omega$ mm on N-face GaN/AlGaN HEMTs with regrown InGaN capped with InN [5], and $R_c \sim 0.06\ \Omega$ mm on metal-face GaN/AlN/

GaN HEMTs with regrown n^+-GaN [6]: and both by molecular beam epitaxy (MBE). To this end we have investigated MBE ohmic regrowth for InAlN/GaN HEMTs. Our preliminary results showed a promising contact resistance of $0.4\ \Omega$ mm by regrowing n^+-GaN ohmics (compromised by a poor ohmic metal deposition process in this study). DC performance of InAlN/AlN/GaN HEMTs with these regrown contacts are presented and discussed along with strategies for improvements.
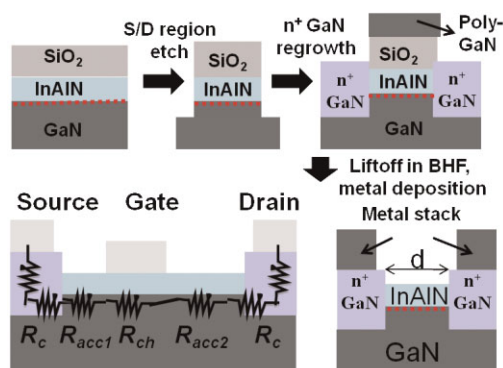
2 Device structure and fabrication The InAlN/AlN/GaN HEMT structure was grown by metal-organic chemical vapour deposition (MOCVD) on SiC substrate at IQE RF LLC. It consists of 2-μm semi-insulating GaN, 1.5 nm AlN spacer and 5.6 nm $In_{0.17}AlN$ barrier. A sheet charge of $2 \times 10^{13}\ cm^{-2}$, electron mobility of 1210 cm^2/Vs, and sheet resistance of 257 Ω/sq were determined by the Hall effect measurement at room temperature on the as-grown wafer. A 270 nm thick SiO_2 mask was first deposited using plasma-enhanced chemical vapour deposition (PECVD) and then patterned by buffered HF. With the patterned SiO_2 as mask InAlN/AlN/GaN was etched down for 30 nm in the ohmic region using BCl_3/Cl_2 inductively couple plasma
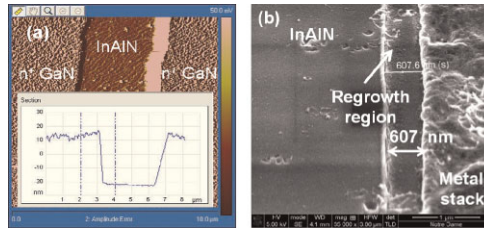
reactive ion etch (ICP-RIE). After solvent clean, the patterned sample was loaded in a Veeco 930 MBE system equipped with standard effusion cells for Ga, Si and N_2 plasma source. Heavily doped GaN:Si of 60 nm was then grown at a substrate thermocouple temperature of 630 °C. During regrowth the Ga flux was modulated while keeping the N-flux constant, which was found to enhance lateral epitaxial growth thus promoting intimate contact between the 2DEG channel and regrown material [10]. Polycrystalline GaN deposited on top of the SiO_2 mask during regrowth was lifted off by BHF. Ohmic contacts were formed by electron-beam evaporation of Ti/Al/Ni/Au: the contacts were later annealed at 850 °C for 30 s in N_2. The mesa-isolation was realized using Ar/BCl$_3$/Cl$_2$ plasma in an ICP-RIE system. Electron-beam lithography was used to define Ni/Au gates. Finally, the devices were passivated with 140 nm PECVD SiN. The schematic of this process flow is shown in Fig. 1.

The surface morphology of regrown n$^+$-GaN in the source/drain region and that on the semi-insulating GaN control sample was monitored by atomic force microscopy (AFM). The RMS values were found to be 2.72 and 1.56 nm over $2 \times 2\,\mu m^2$ scans, respectively. The rough surface indicates there is room for regrowth optimization. A sheet resistance of 52 Ω/sq, charge density of $2 \times 10^{15}\,cm^{-2}$ and mobility of 60 cm^2/Vs were obtained by room temperature Hall effect measurements for the control sample. Shown in Fig. 2 is the AFM amplitude image of the source-channel-drain region after the SiO_2 mask together with GaN deposited on the mask was removed in BHF. Atomic step features on the InAlN surface can be clearly seen; from the AFM height scans no gaps could be discerned between the regrown region and InAlN channel, and the regrown source/drain is ~30 nm above the InAlN channel. Also shown in Fig. 2 is the scanning electron microscope (SEM) image of the regrown ohmic region with contact metal stack. SEM was used to determine the InAlN channel length, i.e. the gap size d, used in the transmission line method (TLM) measurements.

Degradation of 2DEG transport properties was observed upon un-optimized PECVD SiO_2 deposition while the MBE

Figure 2 (online color at: www.pss-a.com) (a) AFM $10 \times 10\,\mu m^2$ amplitude image of the source-channel-drain region after the SiO_2 mask was removed, showing atomic steps on the InAlN channel; the inset is a height line scan. (b) SEM image of the regrown ohmic region with contact metal.

regrowth was confirmed not to adversely affect the 2DEG properties in a separate study. The Hall effect measurements show that after ohmic metal deposition without SiN passivation, the 2DEG concentration and mobility were $2.0 \times 10^{13}\,cm^{-2}$ and 766 cm^2/Vs, respectively; and that under the gate ($V_{gs} = 0\,V$) the 2DEG concentration and mobility were $1.7 \times 10^{13}\,cm^{-2}$ and 845 cm^2/Vs, respectively.

3 Results and discussion Shown in Fig. 3 are results from the same TLM set ($100 \times 100\,\mu m^2$ contact pads) before and after SiN passivation. Contact resistance R_c of $0.40 \pm 0.23\,\Omega$ mm and sheet resistance R_{sh} of $425 \pm 27\,\Omega$/sq were extracted from the least square linear fitting of the total resistance for different TLM gap distances – defined by the edges of regrown n$^+$GaN. Therefore, the presented R_c here consists of three components: metal/n$^+$-GaN resistance, n$^+$-GaN resistance (between the ohmic metal and regrowth edges) and n$^+$-GaN/2DEG resistance. After SiN passivation, the extracted R_c increased to $0.72 \pm 0.33\,\Omega$ mm and R_{sh} decreased to $382 \pm 38\,\Omega$/sq. The relatively large scatter in the data most likely stems from the poor ohmic metal deposition process in this study, where the photoresist residue after lithography was found not completely removed prior to the metal deposition. Unfortunately, the mask set used in this study disallows extraction of the metal/n$^+$-GaN
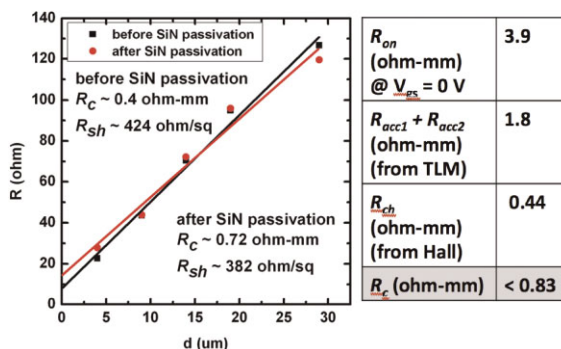

Figure 1 (online color at: www.pss-a.com) Schematic of (top) process flow and (bottom) resistance distribution in a HEMT.

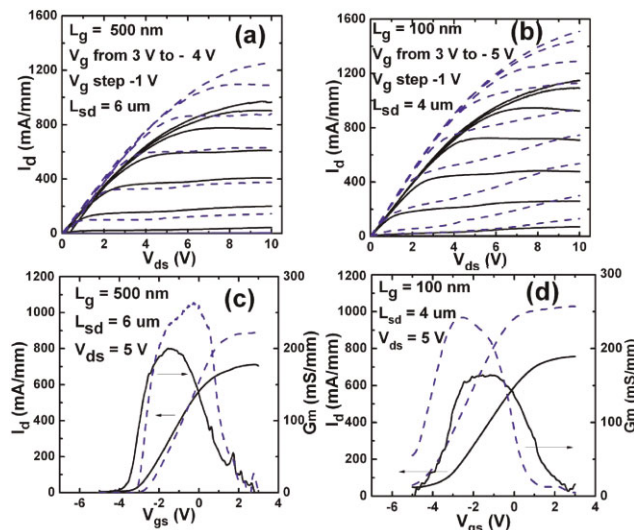**Figure 3** (online color at: www.pss-a.com) (Left) TLM results of regrown contacts before and after SiN passivation. (Right) Estimated R_c from a 500-nm gate length HEMT.

Phys. Status Solidi A **208**, No. 7 (2011)

1619

Original

Paper

Figure 4 (online color at: www.pss-a.com) Common-source characteristics and transfer curves of InAlN HEMTs with regrown contacts before (black solid) and after (blue dotted) passivation: (a, c) $L_g = 500$ nm and (b, d) $L_g = 100$ nm.

contact resistance thus further interrogation of the regrowth interface. However, the metal/n$^+$-GaN resistance is believed to be a substantial portion of the total R_c. Despite this mishap, the data show that ohmic contacts to the 2DEG are successfully realized; and that SiN passivation leads to R_c increase and R_{sh} decrease, which has been also observed in the alloyed ohmic contacts to InAlN HEMTs.

DC characteristics of regrown contact HEMTs with 50 µm gate width are plotted in Fig. 4 for 500 nm ($L_{SD} = 6$ µm) and 100 nm ($L_{SD} = 4$ µm) gate lengths. For 500 nm gate length HEMTs, the maximum drain current density at $V_{gs} = 3$ V increased from 965 to 1256 mA/mm and the peak extrinsic transconductance at $V_{ds} = 5$ V increased from 200 to 264 mS/mm after SiN passivation. For shorter gate length of 100 nm, the maximum drain current density at $V_{gs} = 3$ V increased from 1148 to 1509 mA/mm and the peak extrinsic transconductance at $V_{ds} = 5$ V increased from 164 to 242 mS/mm. The device 3-terminal breakdown voltage V_{br} was found to be ∼23 V at 1 mA/mm, limited by the gate leakage. It is also noteworthy that the buffer leakage is found to reduce by >10× in the devices with regrown contacts compared to those with conventional alloyed contacts (not shown), most likely because metal spikes along dislocations that form during alloying are minimized [11].

The improvement of output current after SiN passivation is attributed to the increase in 2DEG density by barrier height lowering after SiN deposition. The same phenomenon has been observed in (Al, Ga) N/GaN heterostructures [12]. It is interesting to note that the threshold voltage V_{th} of the 100 nm HEMT shifted to be more negative upon SiN passivation, which can be ascribed to short channel effects due to decrease of the effective gate length upon SiN passivation. However, the positive V_{th} shift in the 500 nm

HEMT requires further scrutinization, which may be induced by strain in SiN. Based on the resistance breakdown in a HEMT shown in Fig. 1b, R_c can also be calculated from HEMT on-resistance R_{on}, access resistance and channel resistance. Shown in Fig. 3 (right) are the resistance components calculated from a 500 nm gate length HEMT with SiN passivation. R_c of no more than 0.83 Ω mm was obtained, which agrees reasonably well with the extracted R_c from the TLM measurements. During device fabrication and MBE regrowth, interface states may be introduced at the regrowth interface between n$^+$ GaN and 2DEG channel thus forming barriers for electron flow. In the future characterization of this regrowth interface will be reported. Lower R_c is expected once regrowth mask, ohmic recess etch and regrowth processes are optimized.

4 Conclusions InAlN/GaN HEMTs with MBE regrown n$^+$ GaN ohmic contacts were fabricated for the first time. The overall device performance in this early study shows promises and further investigations are underway to minimize R_c.

References

[1] U. K. Mishra, L. Shen, T. E. Kazior, and Y. F. Wu, Proc. IEEE **96**, 287 (2008).
[2] R. Wang, P. Saunier, X. Xing, C. Lian, X. Gao, S. Guo, G. Snider, P. Fay, D. Jena, and H. Xing, IEEE Electron Dev. Lett. **31**(12), 1383 (2010).
[3] T. Zimmermann, D. Deen, Y. Cao, J. Simon, P. Fay, D. Jena, and H. Xing, IEEE Electron. Devices Lett. **29**, 661 (2008).
[4] Y. Uemoto, M. Hikita, H. Ueno, H. Matsuo, H. Ishida, M. Yanagihara, T. Ueda, T. Tanaka, and D. Ueda, IEEE Trans. Electron. Devices **54**, 3393 (2007).
[5] S. Dasgupta, Nidhi, D. F. Brown, F. Wu, S. Keller, J. S. Speck, and U. K. Mishra, Appl. Phys. Lett. **96**, 143504 (2010).
[6] I. Milosavljevic, K. Shinohara, D. Regan, S. Bumham, A. Corrion, P. Hashimoto, D. Wong, M. Hu, C. Butler, A. Schmitz, P. J. Wiladsen, and M. Micovic, 68th DRC (2010).
[7] F. Recht, L. McCarthy, L. Shen, C. Poblenz, A. Corrion, J. S. Speck, and U. K. Mishra, 65th DRC (2007).
[8] D. Buttari, A. Chini, G. Meneghesso, E. Zanoni, B. Moran, S. Heikman, N. Q. Zhang, L. Shen, R. Coffie, S. P. DenBaars, and U. K. Mishra, IEEE Electron. Device Lett. **23**, 76 (2002).
[9] D. Selvanathan, L. Zhou, V. Kumar, and I. Adesida, Phys. Status Solidi A **194**, 583 (2002).
[10] Y. Cao's, Ph.D. dissertation, University of Notre Dame (2010).
[11] Y. Dora, A. Chakraborty, S. Heikman, L. McCarthy, S. Keller, S. P. DenBaars, and U. K. Mishra, IEEE Electron. Device Lett. **27**, 529 (2006).
[12] M. Higashiwaki, T. Mimura, and T. Matsui, IEEE Electron. Device Lett. **54**, 1566 (2007).